Supplemental information

TGF-β–Smad signal inhibition through VDR nonclassical pathway suppresses fibrosis

Ichiaki Ito[1], Tsuyoshi Waku[2], Masato Aoki[1], Rumi Abe[3], Yu Nagai[3], Tatsuya Watanabe[1], Yuka Nakajima[1], Ichiro Ohkido[4], Keitaro Yokoyama[4], Hiroyuki Miyachi[5], Toshiyuki Shimizu[2], Akiko Murayama[1], Hiroyuki Kishimoto[1], Kazuo Nagasawa[3], and Junn Yanagisawa[1]

[1]Graduate School of Life and Environmental Sciences / Life Science Center of Tsukuba Advanced Research Alliance, University of Tsukuba, Tsukuba Science City, Ibaraki 305-8572, Japan

[2]Graduate School of Pharmaceutical Sciences, The University of Tokyo, Bunkyo-ku, Tokyo 113-0033, Japan

[3]Department of Biotechnology and Life Science, Faculty of Technology, Tokyo University of Agriculture and Technology, Koganei, Tokyo 184-8588, Japan

[4]Division of Nephrology and Hypertension, Department of Internal Medicine, Jikei University School of Medicine, Minato-ku, Tokyo 1058471, Japan

[5]Graduate School of Medicine, Dentistry and Pharmaceutical Sciences, Okayama University, Kita-ku, Okayama 700-8530, Japan

Supplementary Methods

Renal fibroblasts. Kidneys were harvested from C57BL/6 mice and the tissue was minced using a razor blade before it was treated with trypsin–EDTA solution. Cell suspensions were diluted using DMEM supplemented with 10% FBS and seeded onto a tissue culture plate. For immunostaining, cells were fixed in 4% paraformaldehyde and stained with antibodies against α-SMA (Sigma), type I collagen (Abcam), and vimentin (Sigma).

Western blotting. Cells were lysed in TNE buffer [10 mM Tris-HCl (pH 7.8), 1% Nonidet P-40 (NP-40), 0.15 M NaCl, and 1 mM ethylenediaminetetraacetic acid (EDTA)], and then immunoblotted with the appropriate antibodies. The antibodies used in this study were: Smad2 (Santa Cruz), phospho-Smad2 (Cell Signaling), Smad3 (Abcam), phospho-Smad3 (Biosource), VDR (Perseus Proteomics), PAI-1 (Abcam), α-SMA (Sigma), and β-Actin (Sigma) antibodies. Specific proteins were visualized using an enhanced chemiluminescence (ECL) Western blot detection system (Millipore). Band intensities were quantified using the image J program, normalized relative to the quantity of their respective β-actin bands and expressed as fold values relative to the control in each band.

Immunofluorescence. Cells grown on chamber slides were rinsed twice with phosphate-buffered saline (PBS) (140 mM NaCl, 2.7 mM KCl, 1.5 mM KH_2PO_4, and 8.1 mM Na_2HPO_4) and fixed in 4% paraformaldehyde in PBS for 15 min. After rinsing twice with PBS, the cells were permeabilized in 0.1% Triton X-100 in PBS, blocked with TBS-T buffer containing 0.5% bovine serum albumin and 10% goat serum

for overnight at room temperature. Then the cells were incubated with anti-Smad2 (Santa Cruz), anti-Smad3 (Abcam), and anti-VDR (Santa Cruz) antibodies for 1 hour, stained with AlexaFluor-conjugated secondary antibodies (Invitrogen) for 1 hour and mounted with Vectashield (Vector Laboratories). Immunofluorescence was performed using LSM700 confocal laser scanning microscope (Zeiss).

RNA interference. For transfection of siRNAs, cells at 30-50% confluency were transfected with 20 nM of siRNAs (Invitrogen, 5'-CCCACCTGGCTGATCTTGTCAGTTA-3' and 5'-GGACATGATGGAACCGGCCAGCTTT-3') using Lipofectamine RNAi max (Invitrogen) according to the manufacture's protocol. All siRNAs were purchased from Invitrogen.

Luciferase assay. For luciferase assays, 25 ng of the VDRE-Luc or CAGA-Luc plasmids were cotransfected into HEK-293 cells with expression vector encoding 10 ng of ALK5 TD, 10 ng of wild-type or mutated/truncated VDR, and/or 2.5 ng of RXRα in one well of a 24-well plate. We cotransfected 2.5 ng of the ph-RL-TK vectors as a reference plasmid. Transfection was performed with either PerFectin Transfection Reagent (Genlantis) according to the manufacturers' protocols. Twenty-four hr after transfection, we replaced the culture medium with fresh phenol red-free DMEM containing 0.2% charcoal-stripped FBS, and added ligands to the cells for an additional 24 hr incubation. Luciferase assays were performed using cell extracts according to the manufacturer's protocol (Promega).

ChIP assay. ChIP assay was performed as previously described (1). Cells were cultured as described in real-time RT-PCR, and then added ligands and cultured for 3 hr. 10-cm plates to approximately 80% confluence, and one plate was used for each immunoprecipitation. Cells were fixed with 1% formaldehyde for 15 min at room temperature with swirling. Glycine was added to a final concentration of 0.125 M, and the incubation was continued for an additional 10 min. Cells were washed twice with ice-cold PBS, harvested by scraping, pelleted, and resuspended in SDS lysis buffer [50 mM Tris-HCl, pH 8.1, 1% SDS, 10 mM EDTA, and protease inhibitors (NacalaiTesque)]. Samples were sonicated four times for 15 min each with an interval of 30 s with a UH-50 sonicator (SMT). Samples were centrifuged at 13,200 rpm at 4°C for 15 min. After removal of aliquot (whole-cell extract) as input sample, supernatants were diluted 10-fold in ChIP dilution buffer (16.7 mM Tris-HCl, pH 8.1, 16.7 mM NaCl, 1.2 mM EDTA, 1.1% TritonX-100, 0.01% SDS). Samples were incubated at 4°C overnight with 1 μg of normal rabbit IgG or anti-Smad3 antibody (Abcam). The immuno-complexes were collected with 20 μl of protein G Sepharose beads (GE healthcare) for 1 hr at 4°C with rotation. The beads were washed with the following buffers: low salt wash buffer [0.1% SDS, 1% Triton X-100, 2 mM EDTA, 150 mM NaCl and 20 mM Tris–HCl (pH 8.1)], high salt wash buffer [0.1% SDS, 1% Triton X-100, 2 mM EDTA, 500 mM NaCl and 20 mM Tris–HCl (pH 8.1)] and LiCl wash buffer [0.25 mM LiCl, 1% Nonidet P-40, 1% sodium deoxycholate, 1 mM EDTA and 10 mM Tris–HCl (pH 8.1)]. Finally, the beads were washed twice with 1 ml TE buffer [1 mM EDTA and 10 mM Tris–HCl (pH 8.0)]. The immuno-complexes were then eluted by adding 150 μl elution buffer (10 mM DTT, 1% SDS, 100 mM $NaHCO_3$). The elute was collected and the cross-linking was reversed by adding NaCl to final

concentration of 200 mM and incubating for 6 hr at 65°C. The remaining proteins were digested by adding proteinase K. The DNA was phenol precipitated, ethanol precipitated, and measured by qPCR. The primers for qPCR are listed in Supplementary Table 1. Samples were normalized based on the amount of input DNA (n = 3, each group).

Protein preparation. Recombinant His-tagged Smad2, Smad3, Smad4, Smad3-MH1 (1-132 a.a.), Smad3-MH1L (1-214 a.a.), Smad3-MH2 (226-425 a.a.), Smad3-MH1-ΔH1 (20-132 a.a.), Smad3-MH1-LLAA (1-132 a.a., L15A/L16A), VDR-LBD (118-425 a.a.; internally deleted 165-214 a.a.), VDR-LBD iPr/4P mutant (118-425 a.a., F145A/M226A/R274A), or VDR-LBD 2P mutant (118-425 a.a., M412A/K413A), or GST-fused VDR-LBD (110-427 a.a.) or VDR-LBD-ΔH12 (110-403 a.a.) were overexpressed in *E. coli* BL21(DE3)-RIPL at 20°C for 16 hr as a 6xHis-tagged or GST-fusion protein using a pET28b (Novagen), pET30a (Novagen), or pGEX-4T-1 (Pharmacia) vectors. The soluble fraction of the His-tagged proteins in the *E. coli* lysate was purified on Ni^{2+} affinity column (HisTrap, GE healthcare). For GST pull-down assay and EMSA, His-tagged proteins were further purified by cation- or anion-exchange chromatography (HiTrap SP or HiTrap Q column, respectively, GE healthcare). GST-fusion proteins were purified by a glutathione Sepharose column (GE healthcare).

Computational structural modeling of ligand/VDR-LBD complexes. Ligand-receptor complex modeling was carried out using the docking simulation program in the Molecular Operating Environment (MOE; Chemical Computing Group, Montreal,

Canada) package ver. 2011.10. The protein structure of the VDR-LBD in complex with $1,25(OH)_2D_3$ was downloaded from the PDB (Protein Data Bank) (PDB; 1DB1) and hydrogen atoms were added correctly. All ligands in 2D molecular files were also hydrated and converted to 3D PDB files on MOE. An MMFF94x force field was employed to minimize the potential energy of these hydrated structures. Then, MOE-docking simulation using these optimized ligand and LBD structures were carried out for the modeling of ligand/VDR-LBD complex. Since DLAMs induce the non-agonist VDR conformation, the H12 region stabilized in the agonist position was omitted for calculating DLAM/VDR models.

Supplementary Reference

1. Kajiro M, Hirota R, Nakajima Y, Kawanowa K, So-ma K, Ito I, Yamaguchi Y, Ohie SH, Kobayashi Y, Seino Y, et al. The ubiquitin ligase CHIP acts as an upstream regulator of oncogenic pathways. *Nat Cell Biol.* 2009;11:312-319.

Supplementary Table 1.

Primers for qPCR
For mRNA
mouse PAI-1 gene
Fw: 5’-GCCAGATTTATCATCAATGACTGGG-3’
Rv: 5’-GGAGAGGTGCACATCTTTCTCAAAG-3’
mouse CYP24A1 gene
Fw: 5’-TTTAGACCCGAACGCTGGCTTG-3’
Rv: 5’-TGCTGGTCTTGATTTGGGGGTG-3’
mouse α-SMA gene
Fw: 5’-CTGACAGAGGCACCACTGAA-3’
Rv: 5’-ACGCATGATGGCATGAGGCA-3’
mouse type I collagen gene
Fw: 5’-AAGGAGTTTCATCTGGCCCT-3’
Rv: 5’-AGCAGGTCCTTGGAAACCTT-3’
mouse TGF-β1 gene
Fw: 5’-TATGCTAAAGAGGTCACCCGCG-3’
Rv: 5’-TGCTTCCCGAATGTCTGAC-3’
mouse GAPDH gene
Fw: 5’-TGAGGCCGGTGCTGAGTATGTCG-3’
Rv: 5’-CCACAGTCTTCTGGGTGGCAGTG-3’
human PAI-1 gene
Fw: 5’-GAGACAGGCAGCTCGGATTC-3’
Rv: 5’-GGCCTCCCAAAGTGCATTAC-3’
human CYP24A1 gene
Fw: 5’-GCAGCCTAGTGCAGATTT-3’
Rv: 5’-ATTCACCCAGAACTGTTG-3’
human GAPDH gene
Fw: 5’-AGCCACATCGCTCAGACAC-3’
Rv: 5’-GCCCAATACGACCAAATCC-3’
For ChIP assay
mouse PAI-1 gene upstream region
Fw: 5’-CCAAGAGAAAGCCAGGCCAAC-3’
Rv: 5’-GGTGTTTGGAATTCCCTTCCTCG-3’
mouse a-SMA gene upstream region
Fw: 5’-CAAGTCCTCAGCTAATGGCC-3’
Rv: 5’-GGGGATAAACATCCTAAGCC-3’
human PAI-1 gene upstream region
Fw: 5’- GCAGGACATCCGGGAGAGA -3’
Rv: 5’- CCAATAGCCTTGGCCTGAGA -3’

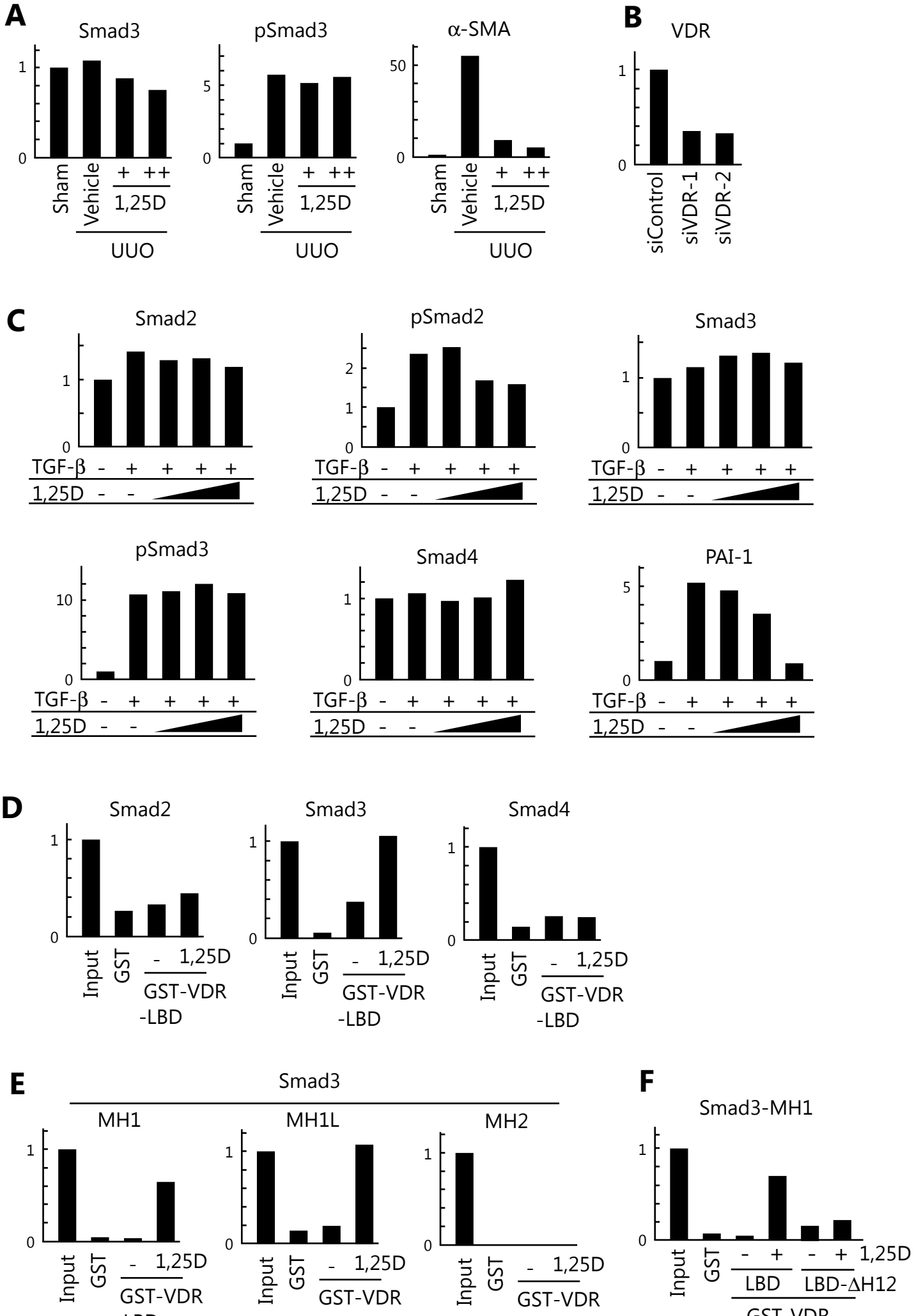
A
Smad3
pSmad3
α-SMA
Sham
Vehicle
+
++
1,25D
UUO
B
VDR
siControl
siVDR-1
siVDR-2
C
Smad2
pSmad2
Smad3
pSmad3
Smad4
PAI-1
TGF-β
1,25D
D
Smad2
Smad3
Smad4
Input
GST
1,25D
GST-VDR
-LBD
E
Smad3
MH1
MH1L
MH2
F
Smad3-MH1
LBD
LBD-ΔH12
GST-VDR-

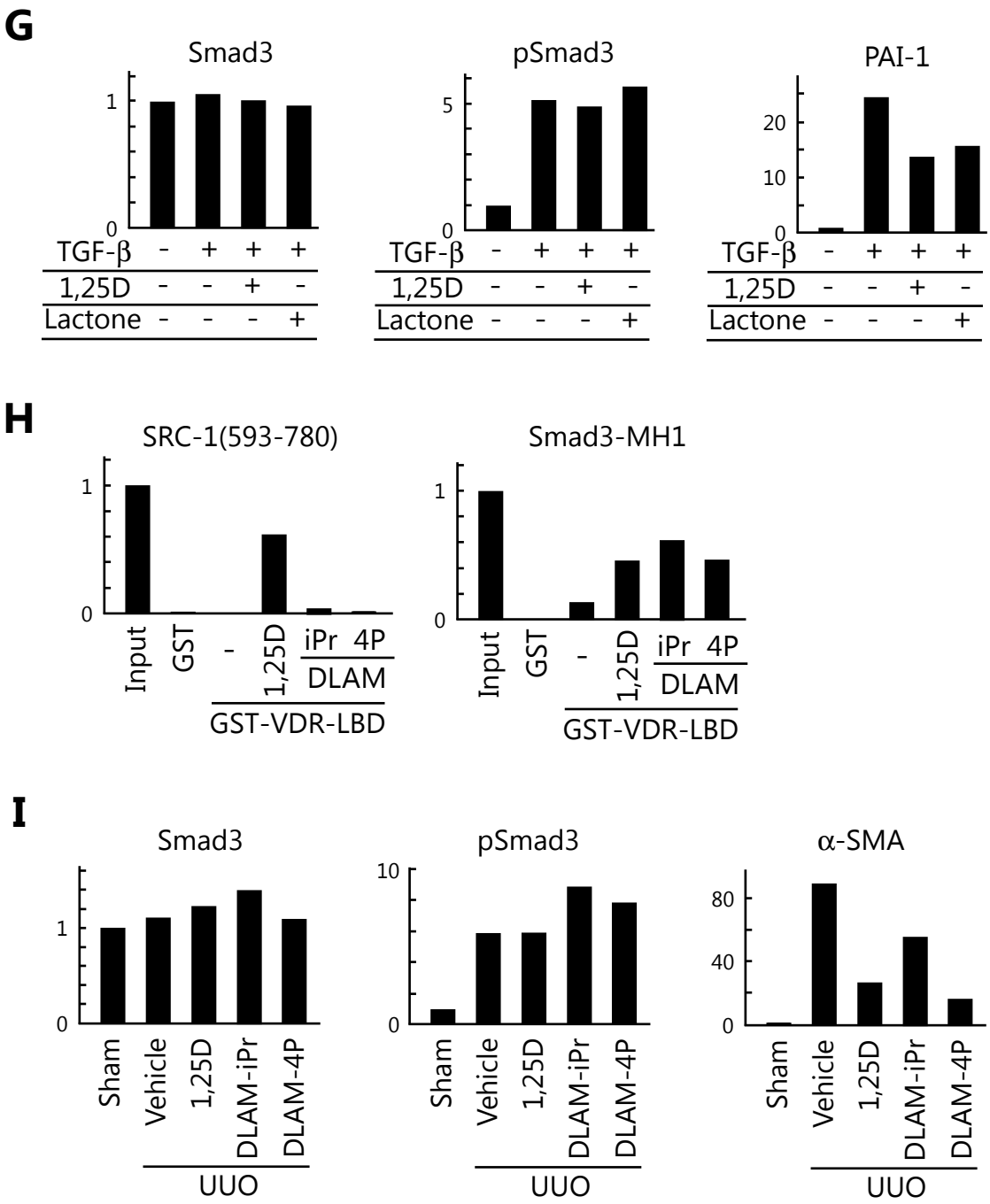

Supplementary Figure 1. Quantification of Western blotting. Graphs represent the quantification of Wester blotting data for Figures 1D (A), 2B (B), 2C (C), 3B (D), 3C (E), 4C (F), 5C (G), 7A (H), and 8B (I).

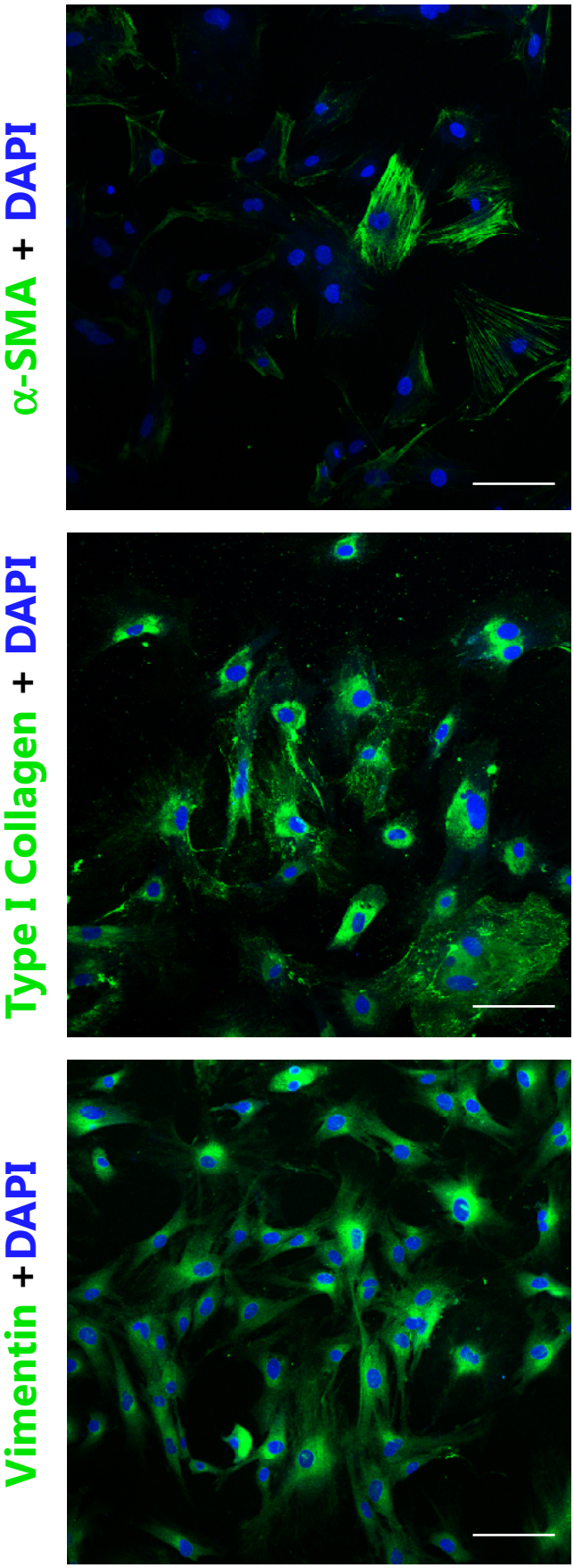

Supplementary Figure 2. Isolated Kidney fibroblasts. Representative photomicrographs of α-SMA, type I collagen, and vimentin-specific immunofluorescence staining of isolated fibloblasts from mice were shown. Scale bars = 100 μm.

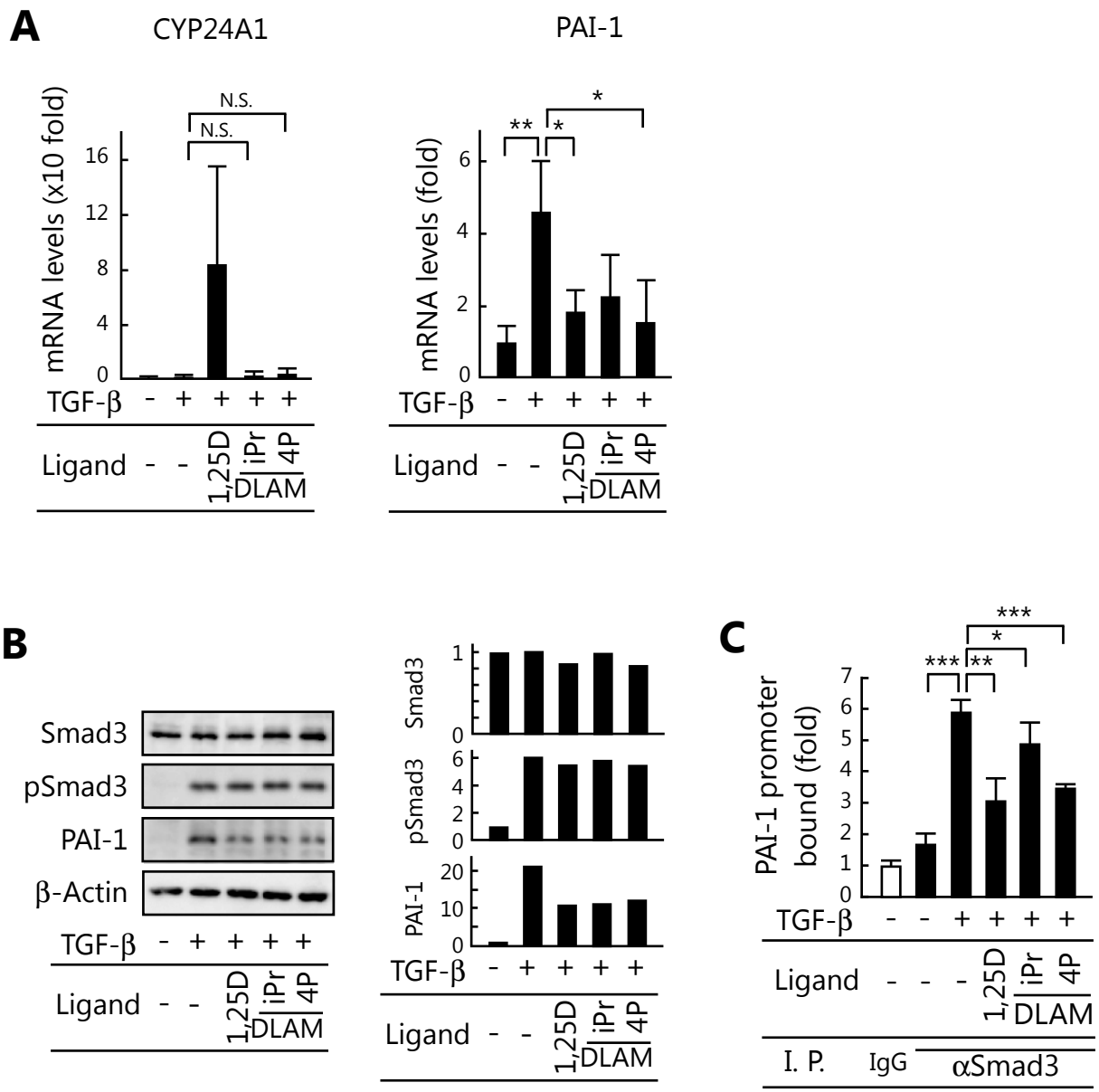

Supplementary Figure 3. DLAM derivatives suppress TGF-β dependent transcription by inhibiting the DNA-binding of Smad3 in human epitherial HK-2 cell line. (A) DLAM -iPr and DLAM-4P suppress TGF-β target gene expression. HK-2 cells were cultured in the presence or absence of TGF-β (5 ng/mL) and 1,25(OH)$_2$D$_3$ (10 nM), DLAM-iPr (1 μM), or DLAM-4P (1 μM). The levels of CYP24A1 and PAI-1 mRNA were determined using qPCR. (B) 1,25(OH)$_2$D$_3$ does not affect the protein levels of Smads. HK-2 cells were cultured in the same conditions with (A). Western blotting was used to examine the levels of Smad3, pSmad3, PAI-1 and β-Actin. Quantified band intensities were represented in right graphs. (C) TGF-β-dependent recruitment of Smad3 to the PAI-1 promoter is inhibited by DLAM-iPr and DLAM-4P. HK-2 cells were cultured in the were cultured in the same conditions with (A). ChIP assays were performed with control IgG or anti-Smad3 antibodies. Immunoprecipitated DNA was examined using qPCR with primers specific for the PAI-1 promoter. Samples were normalized based on the amount of input DNA.
*, P< 0.05; **, P< 0.01; ***, P < 0.001.

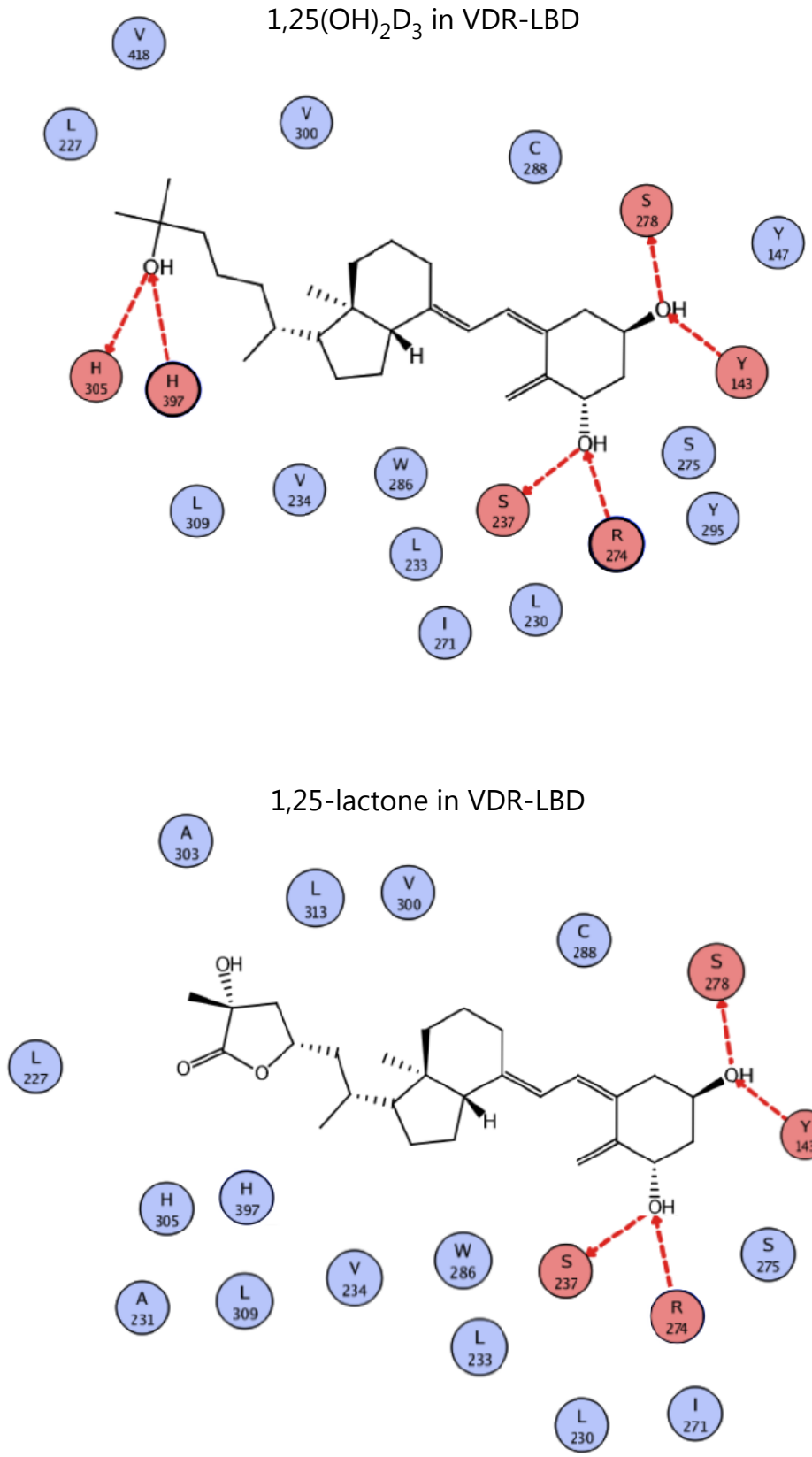

Supplementary Figure 4. Schematic representations of the ligand-receptor interactions. Schematic representation of ligand-receptor interaction, shown in Figure 5D. Residues within 4 angstrom from ligands are shown. Red-colored residues with dashed lines form hydrogen bonds, and blue ones form hydrophobic/val der waals interactions with ligands.

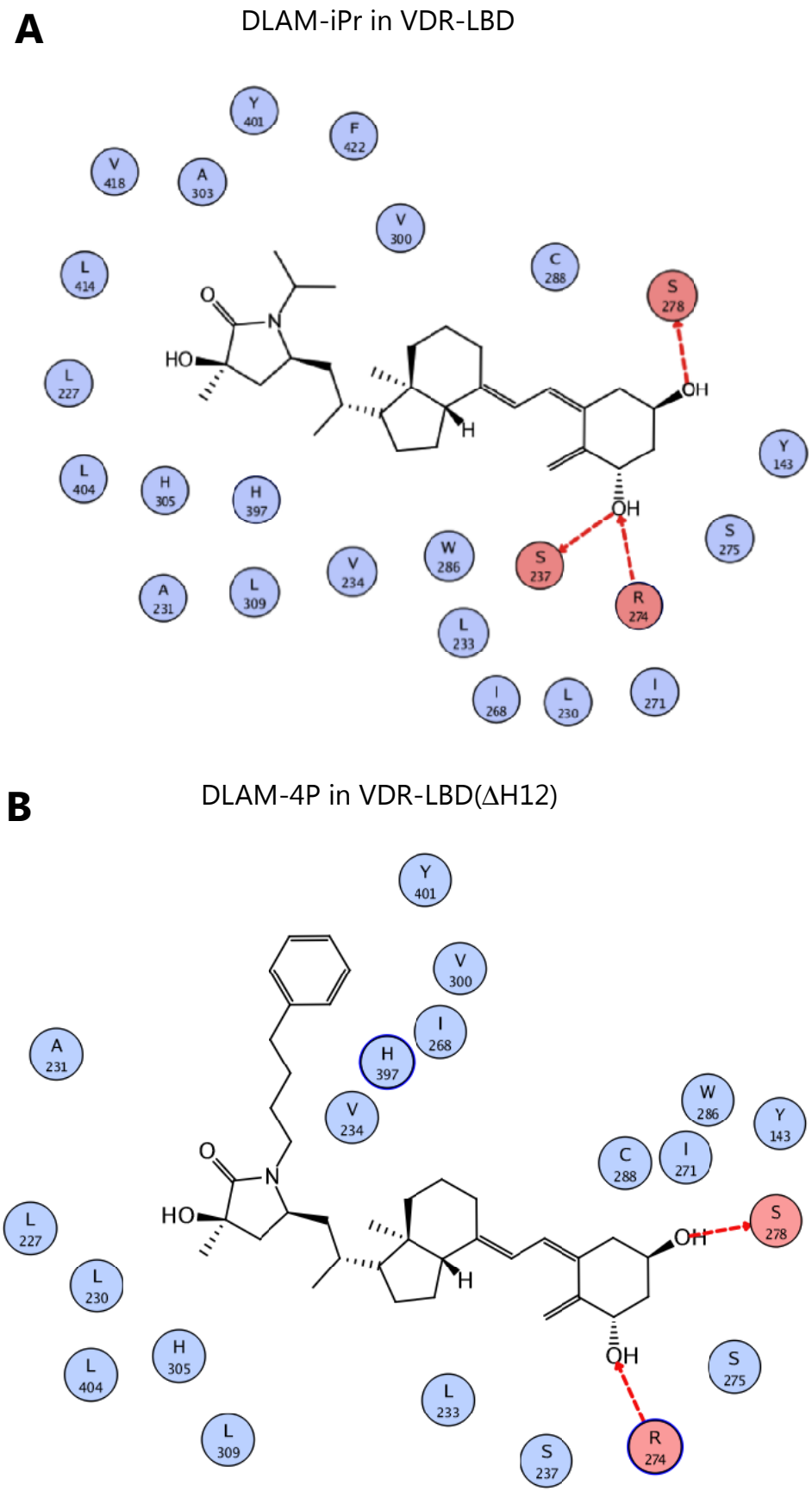

Supplementary Figure 5. Schematic views of DLAM-iPr and DLAM-4P in a ligand binding pocket of VDR. Schematic representation of ligand-receptor interaction, shown in Figure 6B. Docking conformation of DLAM-iPr was superimposed on the VDR-LBD in complex with 1,25(OH)$_2$D$_3$ (A), whereas that of DLAM-4P was on the helix H12-deleted VDR-LBD in complex with 1,25(OH)$_2$D$_3$ (B). Residues within 4 angstrom from ligands are shown, respectively. Red-colored residues with dashed lines form hydrogen bonds, and blue ones form hydrophobic /van der waals interactions with ligands.

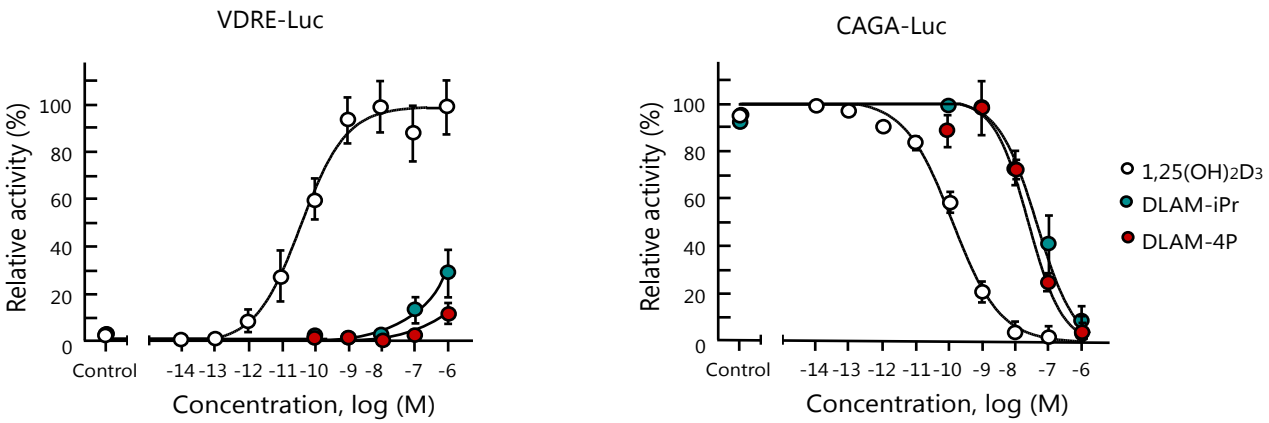

Compounds	Acyivity EC50 (nM)	IC50 (nM)
1,25(OH)2D3	0.0438	0.142
DLAM-iPr	N. D.	30.3
DLAM-4P	N.D.	48.9

Supplementary Figure 6. Characterization of DLAM-iPr and -4P. Plasmids encoding ALK5 TD, and VDR were transfected with reporter plasmids [VDRE-Luc (left) or CAGA-Luc (right)] into HEK293 cells. After culturing transfected cells with or without $1,25(OH)_2D_3$ or DLAM analogues with indicated concentrations for 24 hr, cell extracts were analyzed in luciferase assays. EC_{50} (VDRE-Luc) and IC_{50} (CAGA-Luc) of each ligands were represented in bottom panel.

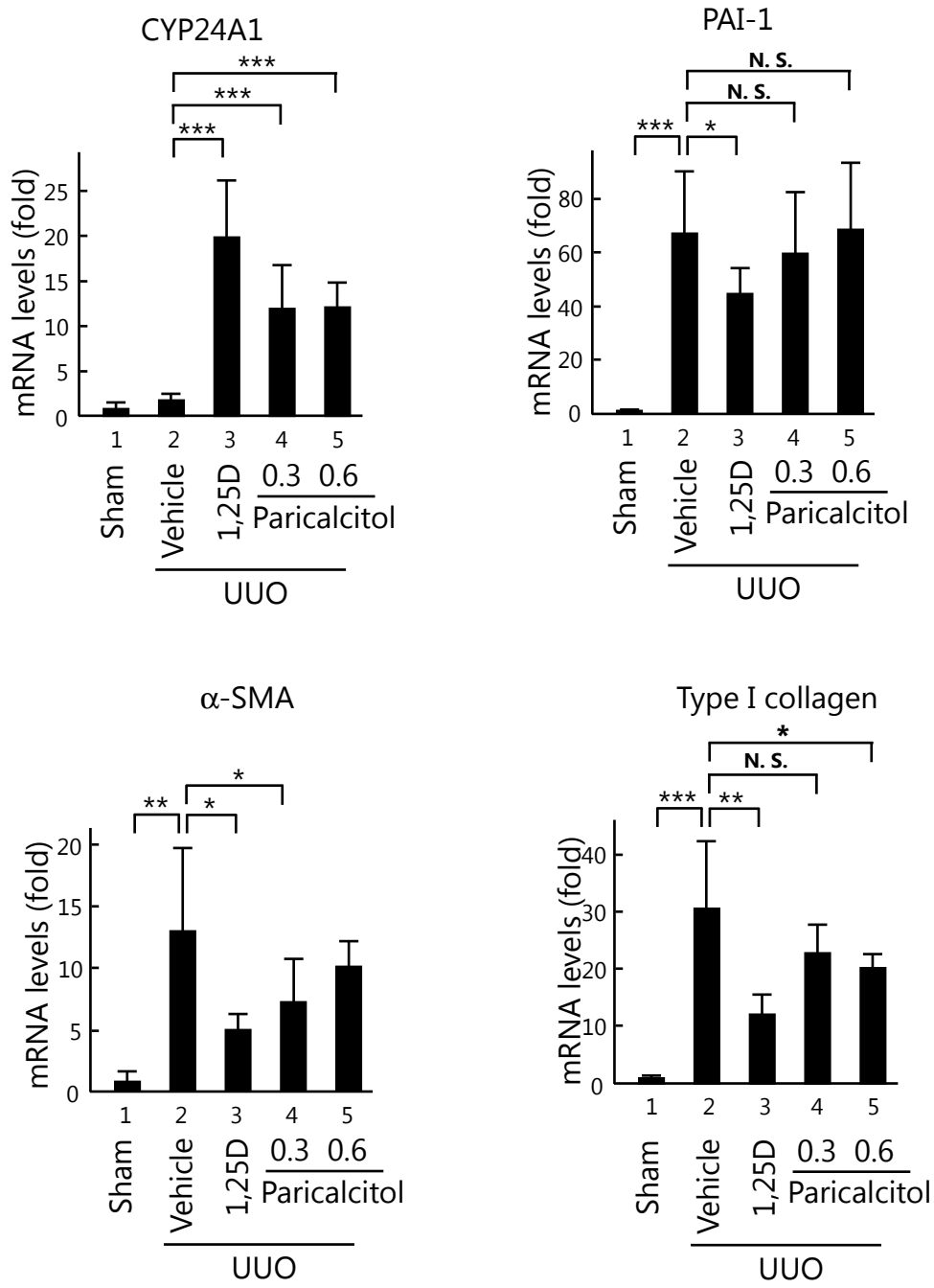

Supplementary Figure 7. Paricalcitol suppresses profibrotic gene expression. RNA isolated from sham-operated or ureteral-obstructed kidneys of mice treated with vehicle, 1,25 $(OH)_2D_3$, paricalcitol was analyzed using qPCR to determine the mRNA levels of the indicated genes.

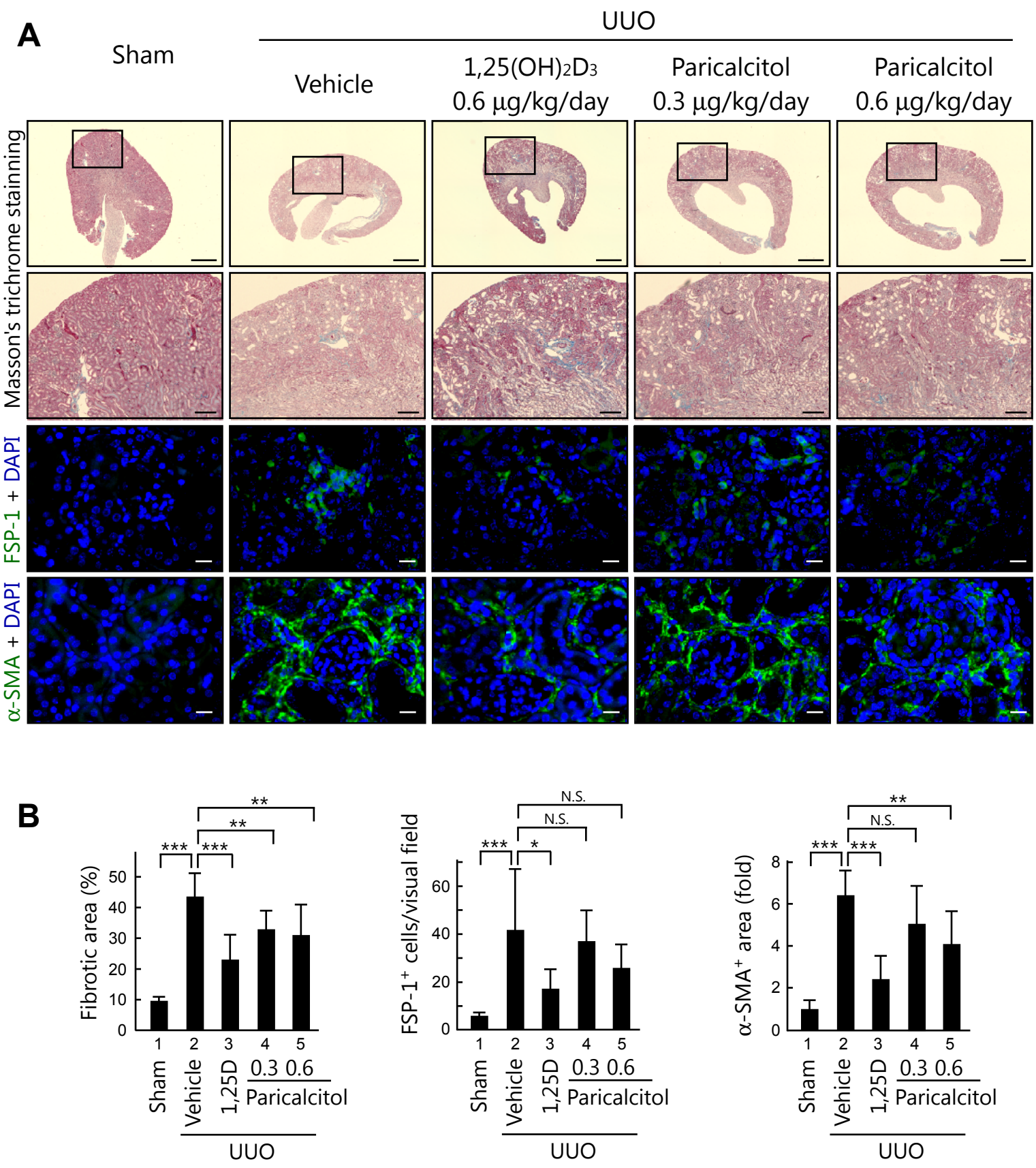

Supplementary Figure 8. Paricalcitol suppresses tubulointerstitial sclerosis. (**A**) Representative photomicrographs of Masson's trichrome staining (top; hole kidney, and 2nd; magnified view of box in top, ×4), FSP-1- and α-SMA- specific immunofluorescence staining (3rd and bottom) of kidney sections from sham-operated or UUO mice injected with vehicle, 1,25(OH)$_2$D$_3$ (0.6 μg/kg/day), and Paricalcitol (0.3 or 0.6 μg/kg/day). Scale bars: 1.0 mm (top); 200 μm (2nd); 20 μm (3rd and bottom). (**B**) Fibrotic, α-SMA-positive or FSP-1-positive areas in stained kidney sections. Data are presented as means ± SD for each treatment group (n = 6, n = 12, or n = 12, each group, respectively).

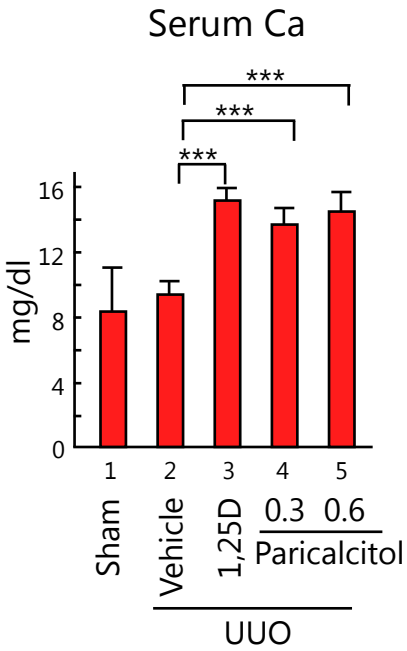

Supplementary Figure 9. Paricalcitol increases serum calcium levels. Average serum calcium concentrations of the indicated treatments of each group.

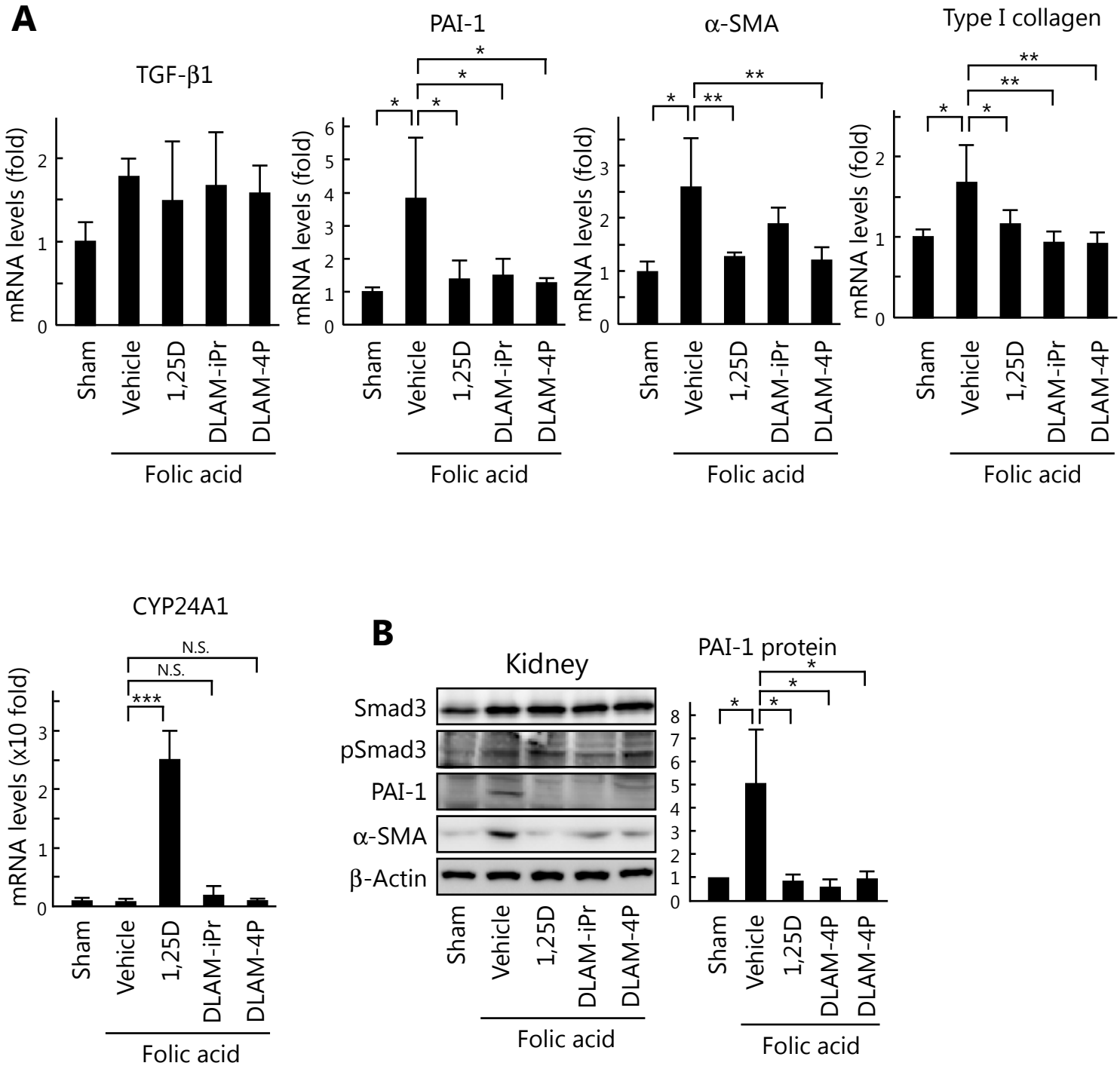

Supplementary Figure 10. DLAM-iPr and -4P suppress the expression of fibrotic genes in short term folic acid-administration model.

(A) DLAM-iPr and -4P suppress the expression of profibrotic genes. We prepared RNA from the kidneys in folic acid and vehicle, 1,25$(OH)_2D_3$ (0.6 mg/kg/day), DLAM-iPr (60 mg/kg/day), or DLAM-4P (60 mg/kg/day) treated mice, and mRNA levels of indicated genes were examined by real-time RT-PCR. (B) Protein levels of indicated factors were examined by Western blotting. The PAI-1 protein levels quantified in each of the treatment groups (n = 3, each group) are shown in the right panel.